CORRECTION POSTED 8 NOVEMBER 2023

SCIENCE ADVANCES | RESEARCH ARTICLE

CHEMSITRY

Uncovering per- and polyfluoroalkyl substances (PFAS) with nontargeted ion mobility spectrometry–mass spectrometry analyses

Kaylie I. Kirkwood-Donelson[1], James N. Dodds[2], Astrid Schnetzer[3], Nathan Hall[4], Erin S. Baker[2]*

Because of environmental and health concerns, legacy per- and polyfluoroalkyl substances (PFAS) have been voluntarily phased out, and thousands of emerging PFAS introduced as replacements. Traditional analytical methods target a limited number of mainly legacy PFAS; therefore, many species are not routinely assessed in the environment. Nontargeted approaches using high-resolution mass spectrometry methods have therefore been used to detect and characterize unknown PFAS. However, their ability to elucidate chemical structures relies on generation of informative fragments, and many low concentration species are not fragmented in typical data-dependent acquisition approaches. Here, a data-independent method leveraging ion mobility spectrometry (IMS) and size-dependent fragmentation was developed and applied to characterize aquatic passive samplers deployed near a North Carolina fluorochemical manufacturer. From the study, 11 PFAS structures for various per- and polyfluorinated ether sulfonic acids and multiheaded perfluorinated ether acids were elucidated in addition to 36 known PFAS. Eight of these species were previously unreported in environmental media, and three suspected species were validated.

INTRODUCTION

Per- and polyfluoroalkyl substances (PFAS) are a class of anthropogenic pollutants comprised of highly fluorinated aliphatic compounds. Their unique properties have been leveraged since the 1950s to create a variety of industrial and household materials with nonstick, repellant, and surfactant characteristics (*1*, *2*). However, these properties also lead to the high potential for toxicity, environmental mobility, bioaccumulation, and environmental persistence due to thermal inertness and resistance to biological breakdown (*3*–*6*). By the 2000s, global concerns were raised regarding historically used long-chain perfluorinated alkyl acids (PFAAs), particularly perfluorooctanoic acid (PFOA) and perfluorooctanesulfonic acid (PFOS). Manufacturers in most developed countries began phasing out legacy compounds including PFOA and PFOS and producing replacement fluorinated alternatives with similar characteristics, such as short-chain PFAAs (perfluoroalkyl carboxylic acids with ≤7 perfluorinated carbons or perfluoroalkyl sulfonic acids with ≤6 perfluorinated carbons) and per- and polyfluoroalkyl ether acids (PFEAs) (*1*, *7*–*9*). Initial studies have demonstrated that these replacements have similar toxicological and environmental implications as their predecessors (*9*–*13*). This shift has resulted in a proliferation of emerging PFAS, whether they are generated as the intended commercial product compounds, their precursors, manufacturing impurities, or degradation products. As of August 2021, the U.S. Environmental Protection Agency's (US EPA) CompTox Chemicals Dashboard PFAS Master List has more than 14,000 entries (*14*). However, the exact number of unique PFAS is difficult to estimate as additional compounds are continually developed and identified. Furthermore, a very small percentage of these chemicals have any publicly available information on their toxicological impacts or presence in the environment.

Most established analytical methods and PFAS monitoring studies focus on legacy PFAS or include only a small subset of emerging compounds. For example, the US EPA methods for PFAS analysis in potable water quantify 14 to 25 unique PFAS with less than half of the targets considered emerging PFAS based on chain length and ether substitution (*15*–*17*). While this provides important and useful information on a rapid time scale, targeted methods cannot capture the growing list of PFAS. Mass balance studies have demonstrated that known PFAS targets account for only 1 to 50% of the total fluorine content of environmental samples (*18*–*21*). Analytical methods enabling the discovery and characterization of PFAS are therefore crucial to better understand the hazards and environmental patterns of previously unknown PFAS. Furthermore, uncovering unknown PFAS can ultimately lead to the commercialization of authentic standards needed for toxicological and quantitative studies, as well as alterations of established targeted methods to monitor for PFAS of emerging concern on regional or global scales. Thus, nontargeted approaches using high-resolution mass spectrometry (HRMS) have been used to detect, identify, and monitor emerging PFAS (*18*). Advances in HRMS instrumentation and coupled front-end separations [e.g., liquid chromatography (LC) and IMS] enable measurements with high resolving power, mass accuracy, and sensitivity. Thus, the resulting platforms are well suited for the identification and monitoring of various chemicals without a priori hypotheses about the species present, publicly available chemical information, or commercially available standards (*22*, *23*).

While putative formulas can be assigned for unknowns using full-scan HRMS data only, fragmentation data are required for structural elucidation of spectral features. A common approach in nontargeted analyses is to collect initial full-scan mass spectrometry (MS)–only data followed by a second analytical run using a targeted

[1]Department of Chemistry, North Carolina State University, Raleigh, NC, USA. [2]Department of Chemistry, University of North Carolina at Chapel Hill, Chapel Hill, NC, USA. [3]Department of Marine, Earth, and Atmospheric Sciences, North Carolina State University, Raleigh, NC,, USA. [4]Department of Marine, Earth, and Atmospheric Sciences, University of North Carolina at Chapel Hill, Morehead City, NC, USA.
*Corresponding author. Email: erinmsb@unc.edu

MS/MS method to fragment features of interest identified in the initial dataset (*24*–*26*). This is a relatively time-consuming approach and limits the opportunity to reinterrogate the same dataset to find additional compounds as chemical databases expand and data analysis software improves over time. Some HRMS platforms can make several MS/MS injections and leverage an iterative exclusion method to exclude ions previously isolated for fragmentation from sequential runs to increase the fragmentation coverage. Alternatively, many nontargeted analyses use methods that collect both precursor and fragmentation information in the same analytical run. This is typically accomplished using data-dependent acquisition (DDA) methods, which select precursor ions for sequential fragmentation in real time based on their relative intensity in the full scan (e.g., the top 10 most intense ions are selected and fragmented). While this approach is highly useful for samples where PFAS are the dominant signals, such as concentrated water collected near point sources (*27*) or aqueous film-forming foams (AFFFs) and other industrial formulations (*28*), it may not successfully select and fragment PFAS when there are more abundant matrix interferences such as biomolecules or polymer contaminants (*18*). Furthermore, DDA is subject to stochastic sampling, meaning it does not reproducibly select the same precursor ions for fragmentation in each sample run, potentially leading to missing data and relative abundance disparities. Data-independent acquisition (DIA) methods can overcome the challenges faced by the two aforementioned methods in that both the precursor and fragmentation information are collected in the same analytical run for all ions regardless of their intensity in the full scan data. A variant of DIA known as all-ions fragmentation (AIF) simultaneously fragments the entire mass/charge ratio (*m/z*) range without any precursor selection by collecting alternating frames of low and high collision energy (CE). AIF has been previously applied to characterize commercial surfactant concentrates (*29*) and find chloroperfluoropolyether carboxylates in New Jersey soil (referred to by the vendor-specific term "MS^E" rather than AIF) (*30*), providing 47 PFAS identifications in the surfactants and 10 in the soil.

A potential limitation of AIF is that the deconvolution of fragments can be challenging when all co-eluting precursors are fragmented in the same scan, whereas MS/MS spectra from DDA and targeted experiments have unambiguous precursors due to the precursor selection process. Using IMS as a front-end separation technique, however, can greatly simplify the deconvolution process. IMS is a gas-phase separation technique that separates ions based on their size, shape, and charge state. Drift tube IMS is an IMS platform in which ions are pulled through a drift tube filled with a buffer gas (e.g., N_2) by a weak electric field following ionization. Smaller ions experience fewer collisions with the buffer gas and therefore migrate faster through the drift tube and have a lower drift time. The ion's drift time is directly correlated to its gas-phase size or collision cross section (CCS; $Å^2$), a molecular descriptor that can be directly compared to previous literature or database values (*31*). IMS separations are rapid, typically occurring on a millisecond timescale; thus, they are easily nested within LC separations (minute time scale) and MS measurements (microsecond time scale). (*32*) Because the IMS separations occur before fragmentation and MS analysis, precursor and fragment drift times are aligned, enabling better deconvolution in AIF schemes. In addition, rather than applying a fixed CE, size-dependent fragmentation can be used wherein the applied CE is higher for lower mobility ions (i.e., larger size or lower charge state). This dynamic, ramped CE approach was initially implemented for peptide ion fragmentation (*33*) but has since been applied to other biomolecules such as lipids (*34*, *35*). In addition to size-based fragmentation capabilities, the addition of IMS greatly benefited other aspects of PFAS nontargeted analyses including isomer separations, matrix distinction, and identification confidence due to CCS validation (*36*–*38*).

In this work, we developed and applied an LC-IMS–collision–induced dissociation (CID)–MS method, leveraging a size-dependent AIF scheme, to detect and fragment PFAS captured by aquatic passive samplers. Figure 1 outlines the nontargeted analysis workflow we used to elucidate the molecular formulas and structures of several unknown PFAS. Following collection of the LC-IMS-CID-MS data, we conduct feature finding to generate a list

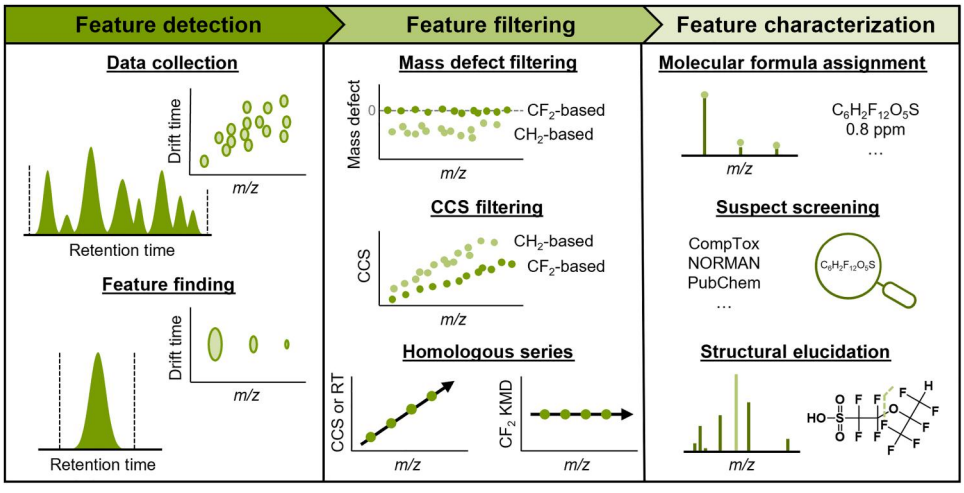

Fig. 1. General workflow for nontargeted per- and polyfluoroalkyl substances (PFAS) discovery using liquid chromatography–IMS–collision-induced dissociation–mass spectrometry (LC-IMS-CID-MS). Feature detection, filtering, and characterization steps are taken to elucidate structures. collision cross section (CCS)– or drift time–related steps are unique to methods using IMS. ppm, parts per million; *m/z*, mass/charge ratio.

of chemical features. These features were defined by specific isotopic distributions and assigned a monoisotopic mass, IMS CCS value, and LC retention time (RT). We then filter the feature list by mass defect or the difference between the nominal and exact mass, as PFAS have characteristically low or negative mass defect values due to the prevalence of fluorine (*39*, *40*). Furthermore, PFAS have distinctly low CCS values or gas-phase sizes compared to hydrocarbon-based molecules of similar mass (*38*). Plotting feature CCS versus *m/z* values allows for rapid filtering of nonhalogenated features, as replacement of a hydrogen with a halogen results in a large mass increase but a relatively small-molecular size difference, as demonstrated by Foster *et al.* (*38*). Last, we investigate the filtered features for potential homologous series containing common repeating units, such as CF_2 groups, by plotting CCS, RT, and CF_2 Kendrick mass defect (KMD) versus *m/z* (*41*–*45*). We then characterize the remaining features with the highest intensity features given the highest priority for investigation. We assign putative molecular formulas using accurate mass and isotopic distribution and then screen for possible structural matches in the US EPA's CompTox PFAS Master List (*14*), the NORMAN Suspect List Exchange (*46*), PubChem, and previous literature pertaining to the fluorochemical manufacturer of interest (*24*, *47*, *48*). Last, we evaluate fragmentation spectra to validate database matches or generate proposed structures. Together, we elucidated structures of several unknown PFAS via the suspect screening matches (if applicable), observed fragments, and related chemicals.

Using this nontargeted analysis workflow, we identified PFAS adsorbed to an aquatic passive sampler deployed downstream from a fluorochemical manufacturer in North Carolina's Cape Fear River. This manufacturer is known to produce a variety of emerging PFEAs such as hexafluoropropylene oxide dimer acid (HFPO-DA, "GenX"). While GenX has been the major focus of the Cape Fear River PFEA contamination, many other structurally similar emerging PFAS have been detected within the river, often at substantially higher abundance (*24*, *47*–*50*). Furthermore, several PFEAs have recently been detected in the serum of (i) individuals with drinking water provided by the Cape Fear Public Utility Authority (*12*), (ii) Cape Fear River fish (*51*), and (iii) alligators living in the Cape Fear River basin and surrounding coastal waters (*52*). It is therefore crucial to investigate unknown PFAS within the river as an initial step toward determining their subsequent environmental and health implications. Furthermore, the nontargeted methodology and analysis workflow used here can be applied to elucidate unique PFAS in environmental and biological media from worldwide contaminated regions.

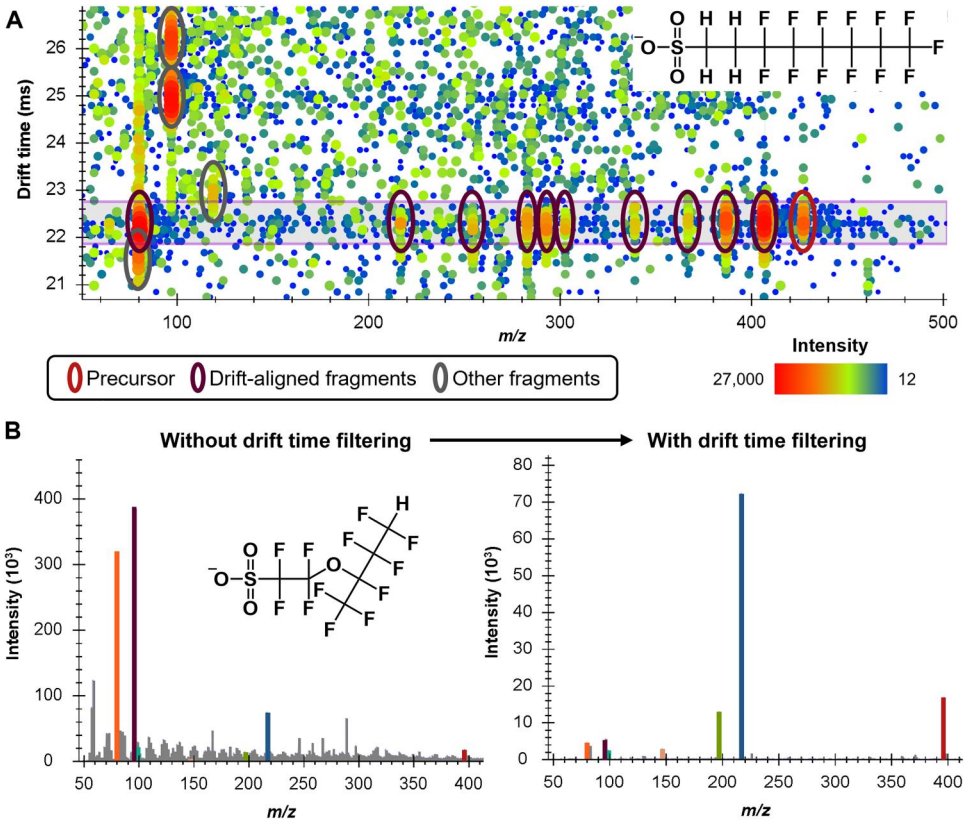

Fig. 2. Drift time alignment and filtering of fragmentation data. (**A**) IMS-collision-induced dissociation–mass spectrometry (IMS-CID-MS) abundance map of 6:2 FTS $[M\text{-}H]^-$ in plant material extract, demonstrating the utility of drift time filtering for the removal of interfering fragments from co-eluting precursors due to the matrix. All signals outside of the purple horizontal box are removed when drift time filtering is applied. (**B**) Comparison of Nafion by-product 6 $[M\text{-}H]^-$ fragmentation spectra without and with drift time filtering where noise from polymer contamination is removed.

RESULTS

Size-dependent fragmentation and alignment

To investigate the optimal CEs for fragmenting PFAS of various chemical structures and sizes (i.e., drift times), 25 PFAS standards spanning 7 PFAS classes underwent fragmentation at fixed CEs ranging from 2 to 60 V (fig. S1). The resulting CE ramp for size-based fragmentation assessing the optimal range for each standard is displayed in figs. S1and S2. While drift times are dependent on both size and charge, PFAS analytes with charge states greater than 1− are rarely observed. Therefore, fragmentation based only on size is discussed here as all analytes were singly charged. Within each class of PFAS, we observed that a larger drift time correlated with a larger or equal optimal CE. Furthermore, as expected, chemical composition also played a role in the optimal CE needed to fragment a given ion. For example, 6:2/8:2 fluorotelomer phosphate diester (6:2/8:2 diPAP) has a larger size or drift time (34 ms) than bis(heptadecafluorooctyl)phosphinic acid [8:8 phosphinic acid (PFPi); 32 ms] yet had a much lower optimal CE of 30 V compared to 60 V. Thus, PFPis require higher energy to induce fragmentation than other PFAS with similar or even larger sizes. Therefore, we optimized the CE to lie within the optimal ranges of as many PFAS standards as possible (fig. S2).

Beyond the ability to use size-dependent fragmentation, IMS is also useful for deconvoluting DIA fragmentation spectra due to drift alignment of precursor and fragment ions. To demonstrate this, we validated the optimized size-dependent fragmentation method with various complex matrices including human serum (*53*), mouse tissue (*54*), and plant material (*36*) from previous studies with known PFAS. Figure 2A displays a typical IMS-CID-MS abundance map for a sample with a complex matrix. Here, the IMS drift times are plotted along the *y* axis, while the *m/z* values are on the *x* axis, and the intensities are shown as a heatmap. In the plant material extract example, the 6:2 fluorotelomer sulfonate (FTS) deprotonated precursor at a drift time of approximately 22.5 ms is circled in red with its drift-aligned fragments circled in maroon. Abundant fragments arising from co-eluting precursors from the matrix at higher or lower drift times are circled in gray. The higher drift time fragments are likely from biomolecules such as lipids, whereas the lower drift time fragment may be from a co-eluting PFAS ion. The purple horizontal box shows the drift time filtering window imposed by Skyline (*55*), which is back-calculated on the basis of the precursor CCS value, instrument resolving power, high-energy drift time offset value (*35*, *56*), and single-field calibration parameters (*57*). All signals outside of this drift time window are removed upon data extraction, similar to signals outside of the precursor *m/z* window based on the resolving power of the mass analyzer, and only the filtered data are displayed on the extracted ion chromatogram (fig. S3). Figure 2B gives another example of the utility of drift time filtering; however, in this case, only the fragmentation spectra are shown without the IMS dimension. In this example, the Nafion byproduct 6 (NBP6) fragmentation spectrum has highly abundant noise due to polymer contamination of the sample. This spectrum would be difficult to interpret, especially if it were an unknown compound without library reference spectra. However, when drift time filtering is imposed in the same fashion as Fig. 2A, the noise is fully removed, and the drift-aligned fragments become readily interpreted.

Nontargeted analysis of aquatic passive samplers

The LC-IMS-MS platform used in this work has previously been applied to nontargeted PFAS analyses; however, structural elucidation was not possible as fragmentation information was not collected (*36*–*38*). Here, we leveraged the optimized LC-IMS-CID-MS method with size-dependent AIF to collect comprehensive precursor and fragmentation data for all PFAS captured by passive samplers commonly used to screen for algal toxins in aquatic systems deployed in an upstream reservoir and directly downstream from a major fluorochemical manufacturer along the Cape Fear River in North Carolina (*58*). The data collected from these samples underwent analysis using the general workflow shown in Fig. 1. We also annotated the data in parallel to this workflow using a targeted LC-IMS-MS Skyline library of >100 PFAS with known *m/z*, RT, and CCS values generated from authentic standards (*38*). Evaluation of the aquatic passive samplers deployed downstream of the fluorochemical manufacturer illustrated 36 known identified PFAS. While these identified PFAS are important from an environmental monitoring perspective, the focus of this application was solely on unknowns; therefore, these features with a library match (table S1) were disregarded in the following discussion. Next, we screened the remaining unknown features of interest to ensure that they were not additional forms of the library matched PFAS, such as dimers, fragments, or additional adducts. We then characterized the remaining unknowns with the highest intensity features given highest priority for elucidation. Additional details on molecular assignment are given in Materials and Methods. Using this workflow, 21 unknown fluorinated features of interest were detected in addition to the 36 detected known, library-matched PFAS (table S1). Of the detected unknowns, 14 unique molecular formulas were assigned comprising 22 total features upon inclusion of isomers. A plot of the CCS versus *m/z* values of all unknown features and known library PFAS is displayed as fig. S4.

None of the unknown features of interest were detected from the "control" aquatic passive sampler deployed in a lake upstream of the fluorochemical manufacturer. At this location, only 20 known PFAS were detected, which is expected given the ubiquitous, persistent nature of legacy PFAS. Furthermore, not all PFAS detected in the downstream sample are produced by the fluorochemical manufacturer, so they may have originated from other sources such as AFFF usage. The unknown features of interest, however, were only detected in the downstream sample and do likely originate from the point source as they are structurally related to the known manufacturing products. A feature initially annotated as the cyclic PFOS analog perfluoroethylcyclohexanesulfonate (PFECHS) was found at similar abundance both upstream and downstream of the fluorochemical manufacturer. This compound has been detected in surface water in the Great Lakes and the North and Baltic Seas, as well as in pine needles collected near Raleigh-Durham International Airport in North Carolina (*36*, *59*, *60*). Upon further investigation, it was clear that while PFECHS was likely present, at least five to seven additional unsaturated PFOS (U-PFOS) isomers were also present (fig. S5). These isomers are likely a mixture of linear and branched PFOS analogs with a single double bond, as they had larger drift times, and therefore larger sizes than the compact cyclic PFECHS. Linear U-PFOS isomers with a double bond between C5 and C6 or between C6 and C7, as well as some potential branched isomers, have previously been detected in human serum and drinking water near an AFFF-contaminated area (*61*). The lack

of LC peak resolution and comprehensive fragmentation did not allow for full deconvolution and annotation of this isomer mixture.

Structural elucidation of unknown PFAS

Upon assessment of the unknown PFAS from the downstream aquatic passive samplers, we elucidated structures for 11 of the 14 assigned molecular formulas (Fig. 3). These structures align well with the findings of surface water analysis from McCord and Strynar from a nearby region of the Cape Fear River approximately 1 year after the deployment of the aquatic passive samplers used here (*24*). This study reported 38 unique molecular formulas, 17 of which were also assigned here as both known and unknown features (table S2). Most of the overlapping compounds were considered known PFAS in this study, including GenX, multiple Nafion by-products (1, 2, 4, 5, and 6) PFO4DA, PFO3OA, hydro-EVE, NVHOS, and per- and polyfluoroalkyl ether sulfonic acid (PFEESA). A similar framework was used to group the proposed candidate structures for unknowns, including polyfluorinated ether sulfonic acids, perfluorinated ether sulfonic acids, and multiheaded perfluorinated ether acids. While both carboxylic and sulfonic acids were found in McCord and Strynar's study (*24*), we elucidated only PFESAs here excluding those with multiple acidic sites. This may be due to the underrepresentation of PFESAs within the library used to initially annotate the data, with 19 per- and polyfluoroalkyl ether carboxylic acid (PFECA) targets and only 7 PFESAs, likely a result of fewer commercially available PFESA standards. This may also be due to the difference in chemical properties and size of sulfonic and carboxylic acids, which can affect passive sampler HP20 resin binding efficiency, extraction efficiency, and ionization efficiency. Furthermore, PFESA features are more apparent, therefore more readily assigned molecular formulas, due to the unique isotopic distribution of sulfur-containing compounds with a relatively high M + 2 signal (95.02% ^{32}S and 4.21% ^{34}S). HP20 is a nonpolar styrene-divinylbenzene adsorbent resin; therefore, the small, relatively polar PFECAs that were highly abundant in McCord and Strynar's surface water analysis, such as 2,2 difluoro-2-(trifluoromethoxy)acetic acid, are unlikely to effectively adsorb. This is a potential limitation of this passive sampler, similar to HLB or C18 stationary phase use for PFAS solid-phase extraction and separation. Further studies are needed to assess the

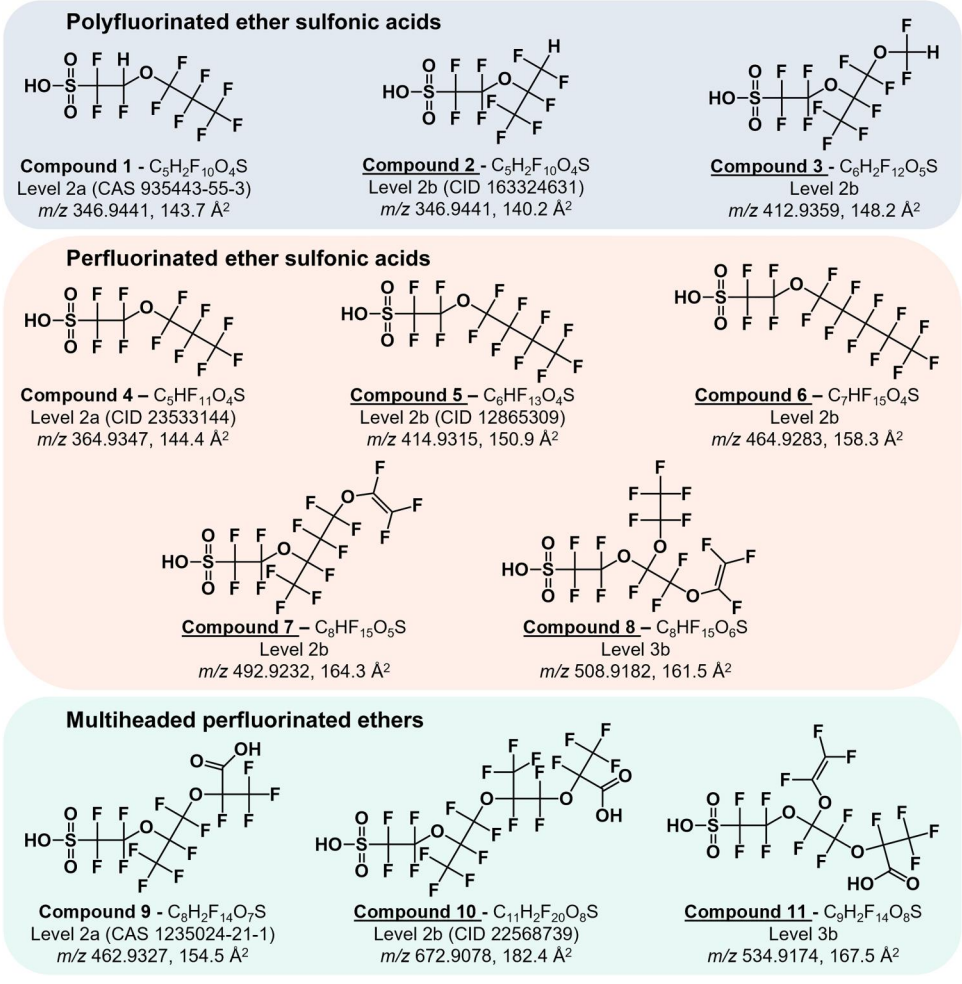

Fig. 3. Elucidated structures of 11 unknowns. Proposed structures, assigned molecular formulas, identification confidence levels (*65*), identifiers (CAS RN or PubChem CID), and experimental descriptors [deprotonated *m/z* and collision cross section (CCS)] are given for each compound. The eight underlined compounds are reported here in environmental media.

HP20 binding affinity for PFAS and characterize the equilibration time and resulting bias introduced by selecting for a fraction of aquatic contamination. Only the most abundant features were characterized here; therefore, several PFECAs may have been present at too low of abundances for structural elucidation due to these possible limitations.

In this study, the first group of elucidated structures, compounds 1 to 3, are polyfluorinated (1H-substituted) ether sulfonic acids (figs. S6 to S8). The production of polyfluorinated ether sulfonic acids (R-OCFH-CF_2-SO_3) and their use as fluoropolymer surfactants are described in patent literature (*62*, *63*). These chemicals are suspected to arise from the manufacturing of Nafion, a polymer used as a cation exchange membrane for various applications such as fuel cells and electrodialysis (*64*). Compound 1, while relatively low in abundance, was also reported by McCord and Strynar with matching fragmentation; thus, it was assigned a confidence level of 2a (*65*). These fragments indicate a hydrogen substitution between the sulfonic acid head group and ether linkage; however, most of the polyfluorinated ether sulfonic acids have hydrogen substitutions on the tail end of the ether, including compounds 2 and 3. Compound 2 was detected by McCord and Strynar; however, no structure was assigned because the diagnostic fragment ion (167 *m/z*) was not detected (*24*). While this fragment is not indicative of the precise hydrogen location, Compound 2 is a $-CF_2$ homolog of NBP6, with one shared fragment and one distinct fragment at the ether linkage differing by *m/z* 50 (49.9968, CF_2). Thus, the hydrogen location of NBP6 was conserved in the proposed structure for Compound 2. Compound 3 is a $-CF_2$ homolog of NBP2 with several shared fragments as well as distinctive fragments at both ether linkages differing by *m/z* 50. A PubChem molecular formula search for this compound returned various isomers, none of which would generate the three most abundant fragments, which each indicate a branched core structure and an OCF_2H tail. Two remaining unknown features assigned putative molecular formulas are likely polyfluorinated ether sulfonic acids given the characteristic sulfur-containing isotopic distribution and the presence of multiple hydrogens (unknowns 1 and 2; table S1). However, they returned no suspect screening matches and did not provide enough fragmentation evidence to fully elucidate their structures.

The second group of elucidated structures are perfluorinated ether sulfonic acids, a common contaminant in this region given the production of Nafion (*24*, *48*, *49*). Compounds 4 to 6 belong to the perfluoro(2-ethyoxyethane)sulfonic acid (PFEESA) homologous series. As displayed in Fig. 4, each additional $+CF_2$ results in an *m/z* increase of 50, along with steady increases in RT (hydrophobicity; Fig. 4A) and CCS (gas-phase size; Fig. 4B). Furthermore, each homolog gave a characteristic ether tail fragment, which also increased by *m/z* 50 intervals (figs. S9 to S11). PFEESA was detected as a known library match, and PFPrESA has previously been detected in water (*24*); however, the larger homologs PFBESA and PFPeESA have not been previously reported in environmental media but have been described in patent literature regarding photoresist polymers. Compound 7 is a $+CF_2$ homolog of NBP1, a perfluorinated byproduct of Nafion production with an unsaturated ether tail ($OCF=CF_2$). An isomer of Compound 7 was reported in McCord and Strynar; however, comparison of the fragments observed here to those observed for NBP1 suggested the additional CF_2 group was located between the two ethers linkages rather than between the sulfonic acid head group and ether linkage (fig. S12) (*24*). Compound 8 is a fragmentation-based candidate structure [level 3b confidence; (*65*)] for an additional perfluorinated NBP. A lack of internal fragmentation made it difficult to assign complete linkage isomerization. The single PubChem molecular formula match for this feature is a linear isomer of compound 8 with repeating OCF_2 units that would not produce any of the diagnostic fragments observed for this compound (fig. S13). In addition to the deprotonated ion, compound 8 also produced a less abundant $[M + H_2O\text{-}H]^-$ adduct (fig. S14).

The final group of elucidated structures are perfluorinated ether acids with multiple acidic sites, specifically PFEAs with both carboxylic and sulfonic acid head groups. These unique compounds are characterized by an overabundance of oxygens (>6) relative to the number of carbons, with at least two hydrogens for both acidic sites. Diagnostic ions for both head groups were observed for each compound. Previous literature has proposed similar structures as unintended side products in fluoropolymer production and degradation (*66*, *67*). Compound 9 was first reported by McCord and Strynar as a precursor of NBP2, where transformation by decarboxylation during production, waste treatment, or naturally in surface waters would yield a compound with a hydrogen at the site of the carboxylic acid (figs. S15 and S16) (*24*). Compound 10 has not previously been reported in environmental media but has also been described in patents regarding photoresist polymers (figs. S17 and S18). In this case, the potential decarboxylated polyfluorinated ether sulfonic acid transformation product was not detected nor has it been described previously. Compound 11 is a fragmentation-based candidate structure [level 3b confidence; (*65*)] for an additional multiheaded perfluorinated ether acid. While it has similar structural components to compound 8, the respective fragmentation spectra indicate differing positions of those components; thus, it is not likely a precursor for this compound; however, it may be a precursor to an isomer of compound 8 that was not detected here (fig. S19). In addition, two remaining unknown features assigned putative molecular formulas are likely perfluorinated ether acids with multiple acidic sites given an overabundance of oxygens (unknowns 3 and 4; table S1). However, they returned no suspect screening matches and did not provide enough fragmentation evidence to fully elucidate their structures.

DISCUSSION

With increasing global restrictions on legacy PFAS because of environmental and health concerns, the introduction of thousands of emerging PFAS has led to the need for nontargeted methods to detect and characterize unknown fluorinated species in the environment. This study demonstrates the effectiveness of a data-independent LC-IMS-CID-MS method using a size-dependent fragmentation scheme to produce informative fragments for all ions regardless of their intensity. We applied this method to aquatic passive samplers deployed upstream and downstream from a fluorochemical manufacturer in North Carolina. The upstream reservoir sample representing background water content contained mostly legacy PFAS, with the exception of a mixture of various cyclic, branched, and linear unsaturated PFOS isomers. Twenty-one unknown fluorinated features of interest were detected in the downstream sample, resulting in 14 unique molecular formulas and 11 candidate structures. These structures include

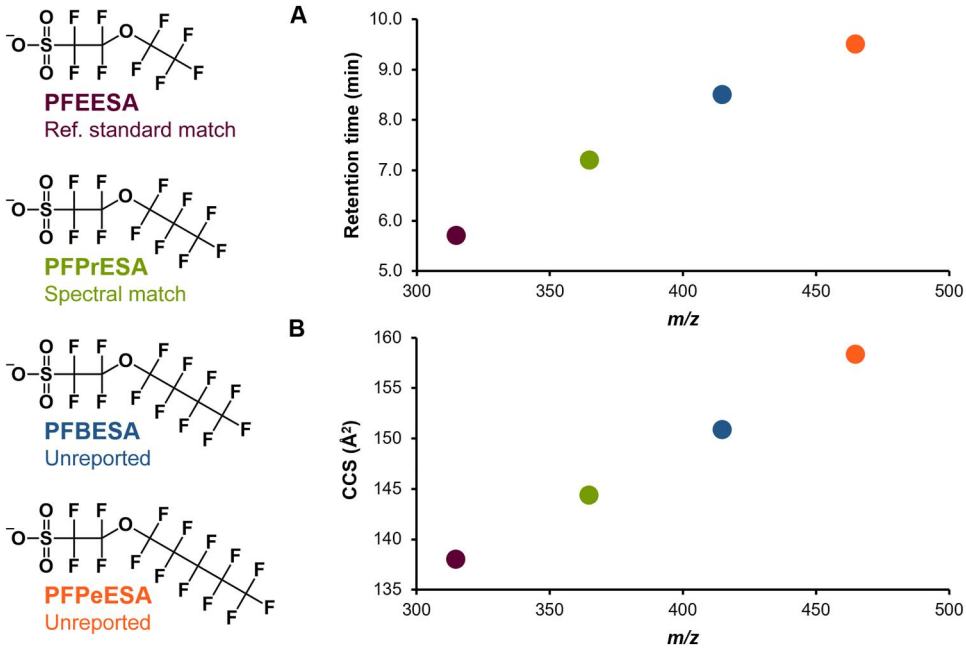

Fig. 4. Perfluoro(2-ethyoxyethane)sulfonic acid (PFEESA) homologous series trends. In addition to conserved fragmentation patterns, each homolog with an additional CF_2 steadily increased in (**A**) retention time (RT) and (**B**) collision cross section (CCS), improving confidence in the previously unreported identifications (PFBESA and PFPeESA).

polyfluorinated ether sulfonic acids, perfluorinated ether sulfonic acids such as the PFEESA homologous series, and multiheaded perfluorinated ether acids, all of which arise from manufacturing of various fluoropolymers. Structurally similar chemicals have been reported and studied along the same river and worldwide (*12*, *13*, *24*, *48*, *51*, *52*, *68*). Further studies to validate the candidate structures proposed here using authentic chemical standards are needed; however, the multidimensional evidence strongly points to these molecular identifications. Following validation, these compounds may be of interest for future monitoring and toxicological studies.

MATERIALS AND METHODS

Materials

Chemical standards were obtained from Wellington Laboratories (Guelph, Canada), including PFAC-MXC (C_4-C_{13}, C_{16}, and C_{18} perfluorocarboxylic acids and C_4-C_{11} perfluorosulfonic acids), 6:2 FTS, HFPO-DA (GenX), PFEESA, 8:8 PFPi, 6:8 PFPi, 6:6 PFPi, 8:2 diPAP, 6:2/8:2 diPAP, and 6:2 diPAP. The complex matrices and aquatic passive samplers were all spiked with the MPFAC-C-ES internal standard mix ($^{13}C_4$-PFBA, $^{13}C_5$-PFPeA, $^{13}C_4$-PFHpA, $^{13}C_5$-PFHxA, $^{13}C_8$-PFOA, $^{13}C_9$-PFNA, $^{13}C_6$-PFDA, $^{13}C_7$-PFUdA, $^{13}C_2$-PFDoA, $^{13}C_2$-PFTeDA, $^{13}C_3$-PFBS, $^{13}C_3$-PFHxS, and $^{13}C_8$-PFOS) before extraction. For extractions and mobile phases, Optima LC-MS–grade methanol, water, and ammonium acetate were obtained from Thermo Fisher Scientific (Hampton, NH).

LC-IMS-CID-MS analysis and CE ramp development

Nontargeted LC-IMS-CID-MS data were collected on an Agilent 6560 IMS-quadrupole time-of-flight (QTOF) coupled with an Agilent 1290 Infinity LC System (Agilent Technologies, Santa Clara, CA). The LC method used here has been previously described (*36*–*38*). Briefly, 2-nl injections were chromatographically separated using a C18 Agilent ZORBAX Eclipse Plus column (2.1 × 50 mm, 1.8 μm) with a flow rate of 0.4 ml/min. Mobile phase A was composed of 5 mM ammonium acetate in water, and mobile phase B (MPB) consisted of 5 mM ammonium acetate in 95:5 methanol/water. The LC gradient with a flow rate of 0.4 ml/min was as follows (% MPB:time): 10%:0 min, 10%:0.5 min, 30%:2 min, 95%:14 min, and 100%:14.5 min held for 2 min. The gradient was followed with a 6-min reequilibration at 10% MPB for a total run time of 22.5 min. An Agilent Jet Stream ESI source (Agilent Technologies, Santa Clara, CA) was operated in negative ionization mode with the source conditions summarized in table S3. IMS-MS settings are summarized in table S3. Agilent ESI tune mix solution (Agilent Technologies, Santa Clara, CA) was directly injected to mass calibrate the instrument and calculate CCS values for the PFAS analytes using a previously described and validated single-field calibration method (*37*). Briefly, tune mix ions with known CCS values served as calibrants for relating measured analyte drift times to CCS values. The LC-IMS-MS method used here has been previously characterized and variation was minimal, with 0 to 0.3% relative standard deviation (RSD) of calculated CCS values and 0- to 0.12-min RT variations, or less than 1% RSD (*37*). All data were collected using a DIA method with an AIF scheme, i.e., alternating frames of low (precursor) and high (fragment) energy scans with no precursor selection. In addition, the aquatic passive sampler samples were reinjected and collected in MS1-only mode with IMS operating in 4-bit multiplexing mode (*69*). All other LC-IMS-MS settings were conserved for these instrument runs (tables S3 and S4) with the exception of a 3900-μs funnel trap fill time and 100-μs trap funnel release time.

To develop and optimize the size- and charge-based CE ramp, neat standard and standard mixture data were collected with fixed CEs. The PFAC-MXC (C_4-C_{13}, C_{16}, and C_{18} perfluorocarboxylic acids and C_4-C_{11} perfluorosulfonic acids) standard mixture was run with fixed CEs of 2, 5, 10, 15, 20, 25, 30, 35, 40, 45, 50, 55, and 60 V. In addition, 6:2 FTS, two PFEAs GenX and perfluoro (2-ethoxyethane)sulfonic acid (PFEESA), three perfluoroalkyl phosphinates (8:8 PFPi, 6:8 PFPi, and 6:6 PFPi) and three perfluoroalkyl phosphate diesters (8:2 diPAP, 6:2/8:2 diPAP, and 6:2 diPAP) were run with fixed CEs of 10, 20, 30, 40, 50, and 60 V. The CE that gave the highest fragment peak area percentage and the greatest number of diagnostic fragments was determined to be the optimal CE for each standard. Acceptable ranges included other CEs above and/or below the optimal value that gave the majority of the same fragments as the optimal CE, each at an acceptable relative abundance (figs. S1 and S2). The optimized CE ramp was then validated using the same standards as used in development, along with extracts from the National Institute of Standards and Technology (NIST) Standard Reference Material (SRM) 1957 (organic contaminants in nonfortified human serum), livers from C57BL/6 mice dosed with PFOA and GenX, and pine needles containing PFAS (*36*, *53*). The optimized CE ramp values are displayed in table S5.

Aquatic passive sampler application

The optimized LC-IMS-CID-MS method was applied to elucidate PFAS captured by a passive sampler (*58*) deployed in the Cape Fear River downstream from a major fluorochemical manufacturer in North Carolina (fig. S20). The passive sampler consisted of HP20 resin between 80-μm Nitex mesh and was deployed at Kings Bluff (N 34.405°, W 78.295°) on the Cape Fear River in July of 2016. A second passive sampler was deployed over the same time period in Jordan Lake (N 35.825°, W 78.998°), a reservoir upstream of the fluorochemical manufacturer, to represent background water content. The passive samplers were frozen at −20°C until extraction and analysis. Before extraction, the passive samplers were pulled from the freezer and thawed and the internal resin was collected, dried overnight, and weighed. A method blank was created with no resin and carried through the extraction alongside the experimental samples. Eight milliliters of methanol containing the MPFAC-C-ES internal standard mix was added to approximately 1 g of resin and vortexed. Two milliliters of water was then added, and the samples were vortexed and then sonicated for 1 hour. The extract was then filtered through a Whatman 0.45-μm glass microfiber syringe filter to remove solid particles from the resin. Last, the extracts were dried under vacuum and reconstituted in 200 μl of 2 mM ammonium acetate in 40:60 methanol/water.

Data analysis

MS1-only data files for the aquatic passive samplers were demultiplexed using the PNNL PreProcessor with a signal intensity threshold of 20 counts (*70*). The demultiplexed data files along with all of the LC-IMS-CID-MS data files were single-field–calibrated for drift time–CCS conversions using Agilent ESI tune mix data in Agilent MassHunter IM-MS Browser 10.0 software (*57*). The CE ramp development and validation data were processed and analyzed within Skyline-daily software (v22.2.1) using a transition list populated with the RT, CCS value, and precursor and product *m/z* values for each PFAS target. Drift time filtering was used with a resolving power of 40 to remove off-target noise and interferences. A high energy ion mobility drift time offset value of −0.2 ms was applied to account for the slightly lower fragment ion drift times compared to the precursor ions due to slightly higher velocities imparted into the smaller fragments from the CID voltage.

The aquatic passive sampler data were initially screened for known PFAS using a targeted LC-IMS-MS library built from authentic standard data containing the class, name, molecular formula, adduct, *m/z*, RT, and CCS values for >100 individual PFAS (*38*). Feature finding was done manually and using Agilent MassHunter IM-MS Browser 10.0 software. The resulting feature list was filtered by identifying features with mass defect and CCS values characteristic of fluorinated chemicals. In addition, features that were present in the method blank and/or the upstream sample collected from a lake upstream of the fluorochemical manufacturer, as well as those determined to be additional features arising from known PFAS (i.e., different adducts, dimers, and in-source fragments), were removed. Features of interest and their retention and drift time–aligned fragments were then imported into Skyline-daily for further analysis. Skyline was used to calculate the observed CCS values of each feature, and then, drift time filtering was used with a resolving power of 50 and high-energy drift time offset value of −0.1 ms to remove noise and interferences in the precursor and fragmentation data. Putative molecular formula assignments were made where possible using MassHunter's formula generator tool. The putative formulas were then input into Skyline to validate the observed isotopic distribution and accurate mass against the theoretical values. In some cases, MassHunter could not generate formulas from the given *m/z* values, or the formulas generated did not match the observed accurate mass and isotopic distribution; thus, some features have no formula reported. For those with assigned formulas, IMS-CID-MS spectra were manually examined for features with putative formulas to attempt to elucidate their molecular structures. The assigned formulas were screened against the EPA's CompTox PFAS Master List (*14*), the NORMAN Suspect List Exchange (*46*), PubChem, and previous literature pertaining to the fluorochemical manufacturer of interest to identify potential known structure matches (*24*, *47*, *48*). Fragment ions were also assigned partial formulas in a similar fashion to the precursors. Assigned formulas for each fragment ion are displayed in the legends of figs. S3, S5 to 13, S15, S17, and S19. In the absence of characteristic fragments or suspect screening matches and related chemicals, only molecular formulas or feature *m/z* values were reported. Characteristic fragments included unique fragments used for structural elucidation and commonly observed perfluoroalkyl sulfonic acid fragments (e.g., SO_3^-, SO_3F^-, $C_nF_nSO_3^-$, and $C_nF_{2n+1}^-$). Each feature was assigned a confidence score based on the PFAS-specific confidence criteria from Charbonnet *et al.* (*65*). Briefly, level 1 identifications are confirmed, level 2 are probable structures, level 3 are candidate structures, level 4 have a determined molecular formula, and level 5 are exact masses of interest (*65*). All identifications here, except for those assigned level 5b (nontarget exact masses of interest), met the criteria of identification by accurate mass, mass defect, and isotopic pattern. PFAS identifications confirmed with a reference standard RT, CCS, and fragmentation spectrum match were assigned a confidence level of 1a. Probable structures with a mass spectral library or literature reference spectrum match were assigned a confidence level of 2a, whereas probable structures with diagnostic fragments but no spectral library match available were level 2b. Fragmentation-based candidate

structures were assigned a confidence level of 3b. Unequivocal molecular formulas with no proposed structure were assigned a confidence level of 4 (table S1). Note that this criterion does not include IMS information, which is a substantial factor in the identification confidence in some cases. (*65*)

Correction (8 November 2023): After publication, the authors alerted the editorial office that they provided the incorrect version of Figure 3 for publication. In the originally published figure, the compound numbers were incorrect and did not correspond to the main text of the paper. The figure has been corrected and the compound numbers listed now correspond with the associated text.

Supplementary Materials

This PDF file includes:

Figs. S1 to S20
Tables S1 to S5

REFERENCES AND NOTES

1. R. C. Buck, J. Franklin, U. Berger, J. M. Conder, I. T. Cousins, P. de Voogt, A. A. Jensen, K. Kannan, S. A. Mabury, S. P. van Leeuwen, Perfluoroalkyl and polyfluoroalkyl substances in the environment: Terminology, classification, and origins. *Integr. Environ. Assess. Manag.* **7**, 513–541 (2011).
2. A. B. Lindstrom, M. J. Strynar, E. L. Libelo, Polyfluorinated compounds: Past, present, and future. *Environ. Sci. Technol.* **45**, 7954–7961 (2011).
3. S. E. Fenton, A. Ducatman, A. Boobis, J. C. DeWitt, C. Lau, C. Ng, J. S. Smith, S. M. Roberts, Per- and polyfluoroalkyl substance toxicity and human health review: Current state of knowledge and strategies for informing future research. *Environ. Toxicol. Chem.* **40**, 606–630 (2021).
4. M. F. Rahman, S. Peldszus, W. B. Anderson, Behaviour and fate of perfluoroalkyl and polyfluoroalkyl substances (PFASs) in drinking water treatment: A review. *Water Res.* **50**, 318–340 (2014).
5. P. Grandjean, R. Clapp, Changing interpretation of human health risks from perfluorinated compounds. *Public Health Rep.* **129**, 482–485 (2014).
6. J. P. Giesy, K. Kannan, Global distribution of perfluorooctane sulfonate in wildlife. *Environ. Sci. Technol.* **35**, 1339–1342 (2001).
7. E. Kissa, Fluorinated surfactants and repellents: Second edition, revised and expanded surfactant science series. *J. Am. Chem. Soc.* **123**, 8882 (2001).
8. M. Scheringer, X. Trier, I. T. Cousins, P. de Voogt, T. Fletcher, Z. Wang, T. F. Webster, Helsingør statement on poly- and perfluorinated alkyl substances (PFASs). *Chemosphere* **114**, 337–339 (2014).
9. Z. Wang, I. T. Cousins, M. Scheringer, K. Hungerbuhler, Fluorinated alternatives to long-chain perfluoroalkyl carboxylic acids (PFCAs), perfluoroalkane sulfonic acids (PFSAs) and their potential precursors. *Environ. Int.* **60**, 242–248 (2013).
10. Z. Wang, I. T. Cousins, M. Scheringer, K. Hungerbuehler, Hazard assessment of fluorinated alternatives to long-chain perfluoroalkyl acids (PFAAs) and their precursors: Status quo, ongoing challenges and possible solutions. *Environ. Int.* **75**, 172–179 (2015).
11. S. Gaballah, A. Swank, J. R. Sobus, X. M. Howey, J. Schmid, T. Catron, J. McCord, E. Hines, M. Strynar, T. Tal, Evaluation of developmental toxicity, developmental neurotoxicity, and tissue dose in zebrafish exposed to GenX and other PFAS. *Environ. Health Perspect.* **128**, 047005 (2020).
12. N. Kotlarz, J. McCord, D. Collier, C. S. Lea, M. Strynar, A. B. Lindstrom, A. A. Wilkie, J. Y. Islam, K. Matney, P. Tarte, M. E. Polera, K. Burdette, J. DeWitt, K. May, R. C. Smart, D. R. U. Knappe, J. A. Hoppin, Erratum: Measurement of novel, drinking water-associated PFAS in blood from adults and children in Wilmington, North Carolina. *North Carolina. Environ. Health Perspect* **128**, 89002 (2020).
13. Y. Pan, H. Zhang, Q. Cui, N. Sheng, L. W. Y. Yeung, Y. Sun, Y. Guo, J. Dai, Worldwide distribution of novel perfluoroether carboxylic and sulfonic acids in surface water. *Environ. Sci. Technol.* **52**, 7621–7629 (2018).
14. A. D. McEachran, J. R. Sobus, A. J. Williams, Identifying known unknowns using the US EPA's CompTox Chemistry Dashboard. *Anal. Bioanal. Chem.* **409**, 1729–1735 (2017).
15. L. Rosenblum, S. C. Wendelken, Method 533: Determination of Per- and Polyfluoroalkyl Substances in Drinking Water by Isotope Dilution Anion Exchange Solid Phase Extraction and Liquid Chromatography/Tandem Mass Spectrometry, US EPA (2019).
16. J. Shoemaker, D. Tettenhorst, Method 537.1: Determination of Selected Per- and Polyfluorinated Alkyl Substances in Drinking Water by Solid Phase Extraction and Liquid Chromatography/Tandem Mass Spectrometry (LC/MS/MS), US EPA (2018).
17. R. A. Brase, E. J. Mullin, D. C. Spink, Legacy and emerging per- and polyfluoroalkyl substances: Analytical techniques, environmental fate, and health effects. *Int. J. Mol. Sci.* **22**, (2021).
18. Y. Liu, L. A. D'Agostino, G. Qu, G. Jiang, J. W. Martin, High-resolution mass spectrometry (HRMS) methods for nontarget discovery and characterization of poly- and per-fluoroalkyl substances (PFASs) in environmental and human samples. *TrAC Trends Anal. Chem.* **121**, 115420 (2019).
19. B. Tan, T. Wang, P. Wang, W. Luo, Y. Lu, K. Y. Romesh, J. P. Giesy, Perfluoroalkyl substances in soils around the Nepali Koshi River: Levels, distribution, and mass balance. *Environ. Sci. Pollut. Res. Int.* **21**, 9201–9211 (2014).
20. P. Wang, T. Wang, J. P. Giesy, Y. Lu, Perfluorinated compounds in soils from Liaodong Bay with concentrated fluorine industry parks in China. *Chemosphere* **91**, 751–757 (2013).
21. Y. Miyake, N. Yamashita, P. Rostkowski, M. K. So, S. Taniyasu, P. K. Lam, K. Kannan, Determination of trace levels of total fluorine in water using combustion ion chromatography for fluorine: A mass balance approach to determine individual perfluorinated chemicals in water. *J. Chromatogr. A* **1143**, 98–104 (2007).
22. M. Krauss, H. Singer, J. Hollender, LC-high resolution MS in environmental analysis: From target screening to the identification of unknowns. *Anal. Bioanal. Chem.* **397**, 943–951 (2010).
23. J. N. Dodds, N. L. M. Alexander, K. I. Kirkwood, M. R. Foster, Z. R. Hopkins, D. R. U. Knappe, E. S. Baker, From pesticides to per- and polyfluoroalkyl substances: An evaluation of recent targeted and untargeted mass spectrometry methods for xenobiotics. *Anal. Chem.* **93**, 641–656 (2021).
24. J. McCord, M. Strynar, Identification of per- and polyfluoroalkyl substances in the cape fear river by high resolution mass spectrometry and nontargeted screening. *Environ. Sci. Technol.* **53**, 4717–4727 (2019).
25. L. Liu, M. Lu, X. Cheng, G. Yu, J. Huang, Suspect screening and nontargeted analysis of per- and polyfluoroalkyl substances in representative fluorocarbon surfactants, aqueous film-forming foams, and impacted water in China. *Environ. Int.* **167**, 107398 (2022).
26. L. A. D'Agostino, S. A. Mabury, Identification of novel fluorinated surfactants in aqueous film forming foams and commercial surfactant concentrates. *Environ. Sci. Technol.* **48**, 121–129 (2014).
27. Y. Wang, N. Yu, X. Zhu, H. Guo, J. Jiang, X. Wang, W. Shi, J. Wu, H. Yu, S. Wei, Suspect and nontarget screening of per- and polyfluoroalkyl substances in wastewater from a fluorochemical manufacturing park. *Environ. Sci. Technol.* **52**, 11007–11016 (2018).
28. K. A. Barzen-Hanson, S. C. Roberts, S. Choyke, K. Oetjen, A. McAlees, N. Riddell, R. McCrindle, P. L. Ferguson, C. P. Higgins, J. A. Field, Discovery of 40 classes of per- and polyfluoroalkyl substances in historical aqueous film-forming foams (AFFFs) and AFFF-impacted groundwater. *Environ. Sci. Technol.* **51**, 2047–2057 (2017).
29. F. Xiao, S. A. Golovko, M. Y. Golovko, Identification of novel non-ionic, cationic, zwitterionic, and anionic polyfluoroalkyl substances using UPLC-TOF-MSE high-resolution parent ion search. *Anal. Chim. Acta* **988**, 41–49 (2017).
30. J. W. Washington, C. G. Rosal, J. P. McCord, M. J. Strynar, A. B. Lindstrom, E. L. Bergman, S. M. Goodrow, H. K. Tadesse, A. N. Pilant, B. J. Washington, M. J. Davis, B. G. Stuart, T. M. Jenkins, Nontargeted mass-spectral detection of chloroperfluoropolyether carboxylates in New Jersey soils. *Science* **368**, 1103–1107 (2020).
31. J. N. Dodds, E. S. Baker, Ion mobility spectrometry: Fundamental concepts, instrumentation, applications, and the road ahead. *J. Am. Soc. Mass Spectrom.* **30**, 2185–2195 (2019).
32. J. C. May, J. A. McLean, Ion mobility-mass spectrometry: Time-dispersive instrumentation. *Anal. Chem.* **87**, 1422–1436 (2015).
33. E. S. Baker, K. Tang, W. F. Danielson 3rd, D. C. Prior, R. D. Smith, Simultaneous fragmentation of multiple ions using IMS drift time dependent collision energies. *J. Am. Soc. Mass Spectrom.* **19**, 411–419 (2008).
34. M. T. Odenkirk, B. M. Horman, J. N. Dodds, H. B. Patisaul, E. S. Baker, Combining micropunch histology and multidimensional lipidomic measurements for in-depth tissue mapping. *ACS Meas. Sci. Au* **2**, 67–75 (2022).
35. K. I. Kirkwood, B. S. Pratt, N. Shulman, K. Tamura, M. J. MacCoss, B. X. MacLean, E. S. Baker, Utilizing Skyline to analyze lipidomics data containing liquid chromatography, ion mobility spectrometry and mass spectrometry dimensions. *Nat. Protoc.* **17**, 2415–2430 (2022).
36. K. I. Kirkwood, J. Fleming, H. Nguyen, D. M. Reif, E. S. Baker, S. M. Belcher, Utilizing pine needles to temporally and spatially profile per- and polyfluoroalkyl substances (PFAS). *Environ. Sci. Technol.* **56**, 3441–3451 (2022).
37. J. N. Dodds, Z. R. Hopkins, D. R. U. Knappe, E. S. Baker, Rapid characterization of per-and polyfluoroalkyl substances (PFAS) by ion mobility spectrometry–mass spectrometry (IMS-MS). *Anal. Chem.* **92**, 4427–4435 (2020).

38. M. Foster, M. Rainey, C. Watson, J. N. Dodds, K. I. Kirkwood, F. M. Fernández, E. S. Baker, Uncovering PFAS and other xenobiotics in the dark metabolome using ion mobility spectrometry, mass defect analysis, and machine learning. *Environ. Sci. Technol.* **56**, 9133–9143 (2022).
39. S. Newton, R. McMahen, J. A. Stoeckel, M. Chislock, A. Lindstrom, M. Strynar, Novel polyfluorinated compounds identified using high resolution mass spectrometry downstream of manufacturing facilities near Decatur, Alabama. *Environ. Sci. Technol.* **51**, 1544–1552 (2017).
40. T. Kind, O. Fiehn, Seven Golden Rules for heuristic filtering of molecular formulas obtained by accurate mass spectrometry. *BMC Bioinformatics* **8**, 105 (2007).
41. Y. Liu, A. D. S. Pereira, J. W. Martin, Discovery of C_5–C_{17} poly- and perfluoroalkyl substances in water by in-line SPE-HPLC-Orbitrap with in-source fragmentation flagging. *Anal. Chem.* **87**, 4260–4268 (2015).
42. I. K. Dimzon, X. Trier, T. Frömel, R. Helmus, T. P. Knepper, P. de Voogt, High resolution mass spectrometry of polyfluorinated polyether-based formulation. *J. Am. Soc. Mass Spectrom.* **27**, 309–318 (2016).
43. J. McCord, M. Strynar, Identifying per- and polyfluorinated chemical species with a combined targeted and non-targeted-screening high-resolution mass spectrometry workflow. *J. Vis. Exp.* **146**, 10.3791/59142, (2019).
44. Y. S. Luo, N. A. Aly, J. McCord, M. J. Strynar, W. A. Chiu, J. N. Dodds, E. S. Baker, I. Rusyn, Rapid characterization of emerging per- and polyfluoroalkyl substances in aqueous film-forming foams using ion mobility spectrometry-mass spectrometry. *Environ. Sci. Technol.* **54**, 15024–15034 (2020).
45. A. Valdiviezo, N. A. Aly, Y. S. Luo, A. Cordova, G. Casillas, M. Foster, E. S. Baker, I. Rusyn, Analysis of per- and polyfluoroalkyl substances in Houston Ship Channel and Galveston Bay following a large-scale industrial fire using ion-mobility-spectrometry-mass spectrometry. *J. Environ. Sci. (China)* **115**, 350–362 (2022).
46. H. M. Taha, R. Aalizadeh, N. Alygizakis, J. P. Antignac, H. P. H. Arp, R. Bade, N. Baker, L. Belova, L. Bijlsma, E. E. Bolton, W. Brack, A. Celma, W. L. Chen, T. Cheng, P. Chirsir, L. Cirka, L. A. D'Agostino, Y. D. Feunang, V. Dulio, S. Fischer, P. Gago-Ferrero, A. Galani, B. Geueke, N. Glowacka, J. Gluge, K. Groh, S. Grosse, P. Haglund, P. J. Hakkinen, S. E. Hale, F. Hernandez, E. M. Janssen, T. Jonkers, K. Kiefer, M. Kirchner, J. Koschorreck, M. Krauss, J. Krier, M. H. Lamoree, M. Letzel, T. Letzel, Q. Li, J. Little, Y. Liu, D. M. Lunderberg, J. W. Martin, A. D. McEachran, J. A. McLean, C. Meier, J. Meijer, F. Menger, C. Merino, J. Muncke, M. Muschket, M. Neumann, V. Neveu, K. Ng, H. Oberacher, J. O'Brien, P. Oswald, M. Oswaldova, J. A. Picache, C. Postigo, N. Ramirez, T. Reemtsma, J. Renaud, P. Rostkowski, H. Rudel, R. M. Salek, S. Samanipour, M. Scheringer, I. Schliebner, W. Schulz, T. Schulze, M. Sengl, B. A. Shoemaker, K. Sims, H. Singer, R. R. Singh, M. Sumarah, P. A. Thiessen, K. V. Thomas, S. Torres, X. Trier, A. P. van Wezel, R. C. H. Vermeulen, J. J. Vlaanderen, P. C. von der Ohe, Z. Wang, A. J. Williams, E. L. Willighagen, D. S. Wishart, J. Zhang, N. S. Thomaidis, J. Hollender, J. Slobodnik, E. L. Schymanski, The NORMAN Suspect List Exchange (NORMAN-SLE): Facilitating European and worldwide collaboration on suspect screening in high resolution mass spectrometry. *Environ Sci Eur* **34**, 104 (2022).
47. M. A. Petre, K. R. Salk, H. M. Stapleton, P. L. Ferguson, G. Tait, D. R. Obenour, D. R. U. Knappe, D. P. Genereux, Per- and polyfluoroalkyl substances (PFAS) in river discharge: Modeling loads upstream and downstream of a PFAS manufacturing plant in the Cape Fear watershed, North Carolina. *Sci. Total Environ.* **831**, 154763 (2022).
48. Z. R. Hopkins, M. Sun, J. C. DeWitt, D. R. U. Knappe, Recently detected drinking water contaminants: GenX and other per- and polyfluoroalkyl ether acids. *J. Am. Water Works Assoc.* **110**, 13–28 (2018).
49. M. Sun, E. Arevalo, M. Strynar, A. Lindstrom, M. Richardson, B. Kearns, A. Pickett, C. Smith, D. R. U. Knappe, Legacy and emerging perfluoroalkyl substances are important drinking water contaminants in the Cape Fear River watershed of North Carolina. *Environ. Sci. Technol. Lett.* **3**, 415–419 (2016).
50. M. Strynar, S. Dagnino, R. McMahen, S. Liang, A. Lindstrom, E. Andersen, L. McMillan, M. Thurman, I. Ferrer, C. Ball, Identification of novel perfluoroalkyl ether carboxylic acids (PFECAs) and sulfonic acids (PFESAs) in natural waters using accurate mass time-of-flight mass spectrometry (TOFMS). *Environ. Sci. Technol.* **49**, 11622–11630 (2015).
51. T. C. Guillette, J. McCord, M. Guillette, M. E. Polera, K. T. Rachels, C. Morgeson, N. Kotlarz, D. R. U. Knappe, B. J. Reading, M. Strynar, S. M. Belcher, Elevated levels of per- and polyfluoroalkyl substances in Cape Fear River Striped Bass (Morone saxatilis) are associated with biomarkers of altered immune and liver function. *Environ. Int.* **136**, 105358 (2020).
52. T. C. Guillette, T. W. Jackson, M. Guillette, J. McCord, S. M. Belcher, Blood concentrations of per- and polyfluoroalkyl substances are associated with autoimmune-like effects in American alligators from Wilmington, North Carolina. *Front. Toxicol.* **4**, 1010185 (2022).
53. A. E. Rodowa, J. L. Reiner, Utilization of a NIST SRM: A case study for per- and polyfluoroalkyl substances in NIST SRM 1957 organic contaminants in non-fortified human serum. *Anal. Bioanal. Chem.* **413**, 2295–2301 (2021).
54. B. R. Rushing, Q. Hu, J. N. Franklin, R. McMahen, S. Dagnino, C. P. Higgins, M. J. Strynar, J. C. DeWitt, Evaluation of the immunomodulatory effects of 2,3,3,3-tetrafluoro-2-(heptafluoropropoxy)-propanoate in C57BL/6 mice. *Toxicol. Sci.*, kfw251 (2017).
55. K. J. Adams, B. Pratt, N. Bose, L. G. Dubois, L. St John-Williams, K. M. Perrott, K. Ky, P. Kapahi, V. Sharma, M. J. Maccoss, M. A. Moseley, C. A. Colton, B. X. MacLean, B. Schilling, J. W. Thompson, Skyline for small molecules: A unifying software package for quantitative metabolomics. *J. Proteome Res.* **19**, 1447–1458 (2020).
56. B. X. MacLean, B. S. Pratt, J. D. Egertson, M. J. MacCoss, R. D. Smith, E. S. Baker, Using skyline to analyze data-containing liquid chromatography, ion mobility spectrometry, and mass spectrometry dimensions. *J. Am. Soc. Mass Spectrom.* **29**, 2182–2188 (2018).
57. S. M. Stow, T. J. Causon, X. Zheng, R. T. Kurulugama, T. Mairinger, J. C. May, E. E. Rennie, E. S. Baker, R. D. Smith, J. A. McLean, S. Hann, J. C. Fjeldsted, An interlaboratory evaluation of drift tube ion mobility–mass spectrometry collision cross section measurements. *Anal. Chem.* **89**, 9048–9055 (2017).
58. R. M. Kudela, Characterization and deployment of Solid Phase Adsorption Toxin Tracking (SPATT) resin for monitoring of microcystins in fresh and saltwater. *Harmful Algae* **11**, 117–125 (2011).
59. A. O. De Silva, C. Spencer, B. F. Scott, S. Backus, D. C. G. Muir, Detection of a cyclic perfluorinated acid, perfluoroethylcyclohexane sulfonate, in the Great Lakes of North America. *Environ. Sci. Technol.* **45**, 8060–8066 (2011).
60. H. Joerss, C. Apel, R. Ebinghaus, Emerging per- and polyfluoroalkyl substances (PFASs) in surface water and sediment of the north and baltic seas. *Sci. Total Environ.* **686**, 360–369 (2019).
61. C. A. McDonough, S. Choyke, K. E. Barton, S. Mass, A. P. Starling, J. L. Adgate, C. P. Higgins, Unsaturated PFOS and other PFASs in human serum and drinking water from an AFFF-impacted community. *Environ. Sci. Technol.* **55**, 8139–8148 (2021).
62. S. Peng, M. H. Hung, C. P. Junk, P. L. Tang. Fluoroalkyl ether sulfonate surfactants, U.S. Patent 7,977,426 B2 (2010).
63. C. P. Junk, M. Harmer, A. Feiring, F. Schadt, Z. Schnepp. Hydrofluoroalkanesulfonic acids from fluorovinyl ethers, U.S. Patent 7,834,209, 2005-06-07 (2006).
64. K. A. Mauritz, R. B. Moore, State of understanding of Nafion. *Chem. Rev.* **104**, 4535–4586 (2004).
65. J. A. Charbonnet, C. A. McDonough, F. Xiao, T. Schwichtenberg, D. Cao, S. Kaserzon, K. V. Thomas, P. Dewapriya, B. J. Place, E. L. Schymanski, J. A. Field, D. E. Helbling, C. P. Higgins, Communicating confidence of per- and polyfluoroalkyl substance identification via high-resolution mass spectrometry. *Environ. Sci. Technol. Lett.* **9**, 473–481 (2022).
66. M. Takasaki, Y. Nakagawa, Y. Sakiyama, K. Tanabe, K. Ookubo, N. Sato, T. Minamide, H. Nakayama, M. Hori, Degradation study of perfluorosulfonic acid polymer electrolytes: Approach from decomposition product analysis. *J. Electrochem. Soc.* **160**, F413–F416 (2013).
67. C. Zhou, M. A. Guerra, Z. M. Qiu, T. A. Zawodzinski, D. A. Schiraldi, Chemical durability studies of perfluorinated sulfonic acid polymers and model compounds under mimic fuel cell conditions. *Macromolecules* **40**, 8695–8707 (2007).
68. Z. Wang, J. C. DeWitt, C. P. Higgins, I. T. Cousins, A never-ending story of per- and polyfluoroalkyl substances (PFASs)? *Environ. Sci. Technol.* **51**, 2508–2518 (2017).
69. J. C. May, R. Knochenmuss, J. C. Fjeldsted, J. A. McLean, Resolution of isomeric mixtures in ion mobility using a combined demultiplexing and peak deconvolution technique. *Anal. Chem.* **92**, 9482–9492 (2020).
70. A. Bilbao, B. C. Gibbons, S. M. Stow, J. E. Kyle, K. J. Bloodsworth, S. H. Payne, R. D. Smith, Y. M. Ibrahim, E. S. Baker, J. C. Fjeldsted, A preprocessing tool for enhanced ion mobility-mass spectrometry-based omics workflows. *J. Proteome Res.* **21**, 798–807 (2022).

Acknowledgments

Funding: This work was supported by NIH grants T32GM133366, R01GM141277, and RM1GM145416; the National Institute of Environmental Health Sciences grants P42ES027704 and P42ES031009; the Environmental Protection Agency cooperative agreement STAR RD84003201; and the NC Sea grant project no. R/16-HCE-2. **Author contributions:** Conceptualization: K.I.K.-D., J.N.D., and E.S.B. Formal analysis: K.I.K.-D., and J.N.D. Methodology: K.I.K.-D., J.N.D., A.S., and N.H. Investigation: K.I.K.-D. and J.N.D. Visualization: K.I.K.-D. and E.S.B. Supervision: E.S.B. Resources: A.S., E.S.B., and N.H. Writing—original draft: K.I.K.-D. and E.S.B. Writing—review and editing: K.I.K.-D., E.S.B., J.N.D., A.S., and N.H. **Competing interests:** The authors declare that they have no competing interests. **Data and materials availability:** All raw LC-IMS-MS and LC-IMS-CID-MS data files are publicly available on MassIVE (MSV000091638). All data needed to evaluate the conclusions in the paper are present in the paper and/or the Supplementary Materials.

Submitted 11 July 2023
Accepted 22 September 2023
Published 25 October 2023
10.1126/sciadv.adj7048